

Scaling laws between the hydrodynamic parameters and molecular weight of linear poly(2-ethyl-2-oxazoline)†

Cite this: *RSC Advances*, 2013, 3, 15108

Xiaodong Ye,^{*ab} Jinxian Yang^a and Jaweria Ambreen^a

Poly(2-ethyl-2-oxazoline) (PEtOx), as an alternative polymer to poly(ethylene glycol), has potential applications in biomedical fields. The hydrodynamic parameters, such as the hydrodynamic radius and sedimentation coefficient, are important to understand its dynamics and properties, including its effect on the interactions between proteins and cells. In this study, we have investigated the hydrodynamic properties and thermodynamic parameters of a series of narrowly distributed PEtOx polymers with molecular weights ranging from 1.3×10^3 to 3.1×10^5 g mol⁻¹, and the scaling laws between them by the use of a combination of analytical ultracentrifugation and laser light scattering. It is found that the sedimentation coefficient ($s_{20,w}$) and hydrodynamic radius ($R_{h,0}$) at infinite dilution scale with molecular weight (M_w) as $s_{20,w} = K_s \times M_w^\alpha = 0.0071$ (S) $\times M_w^{0.462 \pm 0.019}$ and $R_{h,0} = K_{R_h} \times M_w^\beta = 0.0179$ (nm) $\times M_w^{0.539 \pm 0.012}$, respectively.

Received 7th March 2013,
Accepted 20th June 2013

DOI: 10.1039/c3ra41120f

www.rsc.org/advances

Introduction

Polyethylene glycol (PEG) has received great interest in the pharmaceutical industry because PEG is nontoxic, biocompatible and is approved by the FDA.^{1–4} It is well known that the covalent attachment of PEG to proteins (*i.e.* PEGylation) can increase the circulating half-life in blood by increasing the stability of the proteins, as well as by reducing the renal ultrafiltration.^{2–4} Normally, PEGylation can reduce the immunogenicity of some proteins.⁵ However, due to the wide use of PEG in biomedical applications, recently more and more anti-PEG antibodies have been reported.^{6–8} Thus, drug companies are eager to find alternative polymers. Among the alternative polymers, poly(2-ethyl-2-oxazoline) (PEtOx) is a promising candidate because of its low toxicity and immunogenicity.^{9–17} The chemical structures of PEtOx and PEG are shown in Fig. 1.

In order to reduce kidney filtration, the hydrodynamic radius (R_h) of the PEtOx–protein conjugate should be larger than the size of the glomerular basement membrane, which is in the range of 2.5–5 nm.¹⁸ Based on the extensive data from the pharmacokinetic studies of PEG–protein conjugates, a possible way is to replace PEG by PEtOx, which has the same hydrodynamic radius. Recently Armstrong *et al.* found that the

hydrodynamic radii of nonionic polymers and proteins are the principal determinant of their effect on red blood cell aggregation.¹⁹ Moreover, Sim *et al.* have reported that the precipitation efficiency of PEG is mainly determined by the hydrodynamic radius.²⁰ These studies further indicate that knowing the relationship between R_h and the molecular weight of PEtOx can help us to explain the effect of PEtOx on the interactions between cells and proteins. The solution properties of a series of PEtOx polymers with molecular weights ranging from 6.8×10^4 g mol⁻¹ to 9.14×10^5 g mol⁻¹ in THF have been studied by light scattering and viscometry.²¹ While most biomedical applications of PEtOx are in aqueous systems, the aqueous solution properties of PEtOx with a wide range of molecular weights, taking into account the hydrodynamic radius, need to be examined systematically.

In this article, a series of PEtOx polymers with molecular weights from 1.3×10^3 to 3.1×10^5 g mol⁻¹ was obtained by the fractionation of a linear commercial PEtOx sample by gel

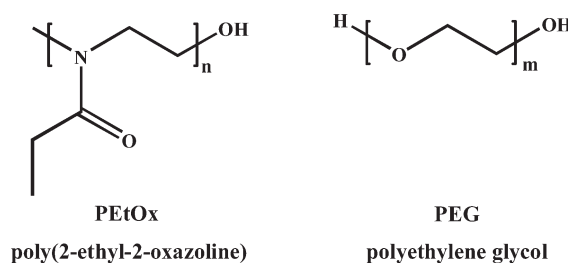


Fig. 1 Chemical structures of PEtOx and PEG.

^aHefei National Laboratory for Physical Sciences at the Microscale, Department of Chemical Physics, University of Science and Technology of China, Hefei, Anhui 230026, China. E-mail: xdy@ustc.edu.cn

^bCAS Key Laboratory of Soft Matter Chemistry, University of Science and Technology of China, Hefei, Anhui 230026, China

† Electronic supplementary information (ESI) available. See DOI: 10.1039/c3ra41120f

permeation chromatography (GPC) or by the cationic ring-opening polymerization of the monomer 2-ethyl-oxazoline. Both analytical ultracentrifugation (AUC) and laser light scattering (LLS) were used to characterize the PEtOx samples. For two linear PEtOx samples with lower molecular weights, both AUC and LLS give similar results regarding the R_h and weight-average molecular weight (M_w). However, because of the low scattering intensity, the concentration of PEtOx used in the LLS experiments was much higher than that used in AUC to obtain reliable results. Possibly for the same reason, Sung and Lee did not report the hydrodynamic radius of PEtOx samples with molecular weights of less than $1.41 \times 10^5 \text{ g mol}^{-1}$ in THF.²¹ Our objective is to understand the scaling of the molecular weight-dependent hydrodynamic parameters of PEtOx in aqueous solution.

Experimental

Materials

Linear poly(2-ethyl-2-oxazoline), with a weight-average molar mass of $500\,000 \text{ g mol}^{-1}$, was purchased from the Sigma-Aldrich Company, Inc. and used as received as a starting material for fractionation. The commercial linear PEtOx sample was carefully fractionated by GPC. Briefly, 50 μL of PEtOx tetrahydrofuran (THF) solution with a concentration of 20 mg mL^{-1} was injected into steam from a sample loop. According to the principle of GPC, it takes a shorter time for the high-molecular-weight polymers to reach the column outlet. Fractions were collected at 1 mL intervals from the chromatography. The same procedure was repeated ten times to obtain sufficient samples. Then, the THF solvent was evaporated under reduced pressure. The aqueous solution of each PEtOx fraction was prepared by dissolving the PEtOx fraction in 0.6 mL Milli-Q water. Two PEtOx samples with lower molecular weights were synthesized by the cationic ring-opening polymerization of the monomer 2-ethyl-2-oxazoline. In brief, 2-ethyl-2-oxazoline (99%, Sigma-Aldrich) was dried over calcium hydride and distilled under reduced pressure prior to use. Methyl tosylate (98%, Sigma-Aldrich) was distilled under reduced pressure. Acetonitrile, the reaction solvent, was refluxed with and distilled from alkaline KMnO_4 and KHSO_4 , followed by fractional distillation from calcium hydride. Methyl tosylate, EtOx and acetonitrile were added into a glass tube. After three freeze-vacuum-thaw cycles, the tube was sealed under vacuum and then placed in a thermostat at $80 \text{ }^\circ\text{C}$ for 24 h. The PEtOx-acetonitrile solution was added to sodium carbonate aqueous solution. The mixture was stirred for 16 h at $90 \text{ }^\circ\text{C}$ and extracted three times with chloroform after cooling to room temperature. The organic phases were dried over sodium sulfate and filtered. Then, the solvent was evaporated under reduced pressure and the resultant PEtOx was dried under reduced pressure. The $^1\text{H-NMR}$ spectra of these two PEtOx samples were recorded in CDCl_3 using a Bruker 300 MHz spectrometer.

Laser light scattering

A commercial laser light scattering spectrometer (ALV/DLS/SLS-5022F) equipped with a multi- τ digital time correlator (ALV5000) and a cylindrical 22 mW UNIPHASE He-Ne laser ($\lambda_0 = 632.8 \text{ nm}$) was used. In static LLS,^{22,23} the weight-average molar mass (M_w) and the z-average root-mean square radius of gyration ($\langle R_g^2 \rangle_z^{1/2}$) in a solution from the angular dependence of the excess absolute scattering intensity which is known as the excess Rayleigh ratio [$R_w(q)$] can be obtained by using

$$\frac{KC}{R_w(q)} \approx \frac{1}{M_w} \left(1 + \frac{1}{3} \langle R_g^2 \rangle_z q^2 \right) + 2A_2C \quad (1)$$

where $K = 4\pi^2 n^2 (dn/dC)^2 / (N_A \lambda_0^4)$ and $q = (4\pi n / \lambda_0) \sin(\theta/2)$ with C , dn/dC , N_A , and λ_0 representing the concentration of the polymer, the specific refractive index increment, Avogadro's number and the wavelength of light, respectively. A_2 is the second virial coefficient. The refractive index increment ($dn/dC = (0.161 \pm 0.001) \text{ mL g}^{-1}$) of PEtOx in water was measured with a precise differential refractometer at $20 \text{ }^\circ\text{C}$ and 633 nm .²⁴ In dynamic LLS,²⁵ the Laplace inversion of a measured intensity-intensity time correlation function $G^{(2)}(t, q)$ in the self-beating mode can result in a line-width distribution $G(I)$. For a pure diffusive relaxation, Γ is related to the translational diffusion coefficient D by $\Gamma/q^2 = D$ at $q \rightarrow 0$ and $C \rightarrow 0$, or a hydrodynamic radius $R_h = k_B T / (6\pi\eta D)$ with k_B , T , and η representing the Boltzmann constant, the absolute temperature and the solvent viscosity, respectively. Each PEtOx aqueous solution was repeatedly filtrated using a peristaltic pump (Masterflex[®], Model 77390-00, Cole-Parmer Instrument Co.) and a $0.45\text{-}\mu\text{m}$ hydrophilic PTFE filter.

Sedimentation velocity analysis

Sedimentation velocity assays were performed using a Proteomelab XL-A/XL-I analytical ultracentrifuge (Beckman Coulter Instruments) with an An-60 Ti rotor, one cell assembled with sapphire windows, a double-sector 12 mm length charcoal-filled Epon centerpiece and an interference optics detector. All of the experiments were conducted at $60\,000 \text{ rpm}$ and $20 \text{ }^\circ\text{C}$. $400 \mu\text{L}$ of the PEtOx fraction solution was loaded for measurement with $410 \mu\text{L}$ of water as the reference. Data were collected using the software provided with the instrument, and analyzed using the SEDFIT (version 12p44) program.^{26,27} The partial specific volume (v) of PEtOx in aqueous solution was measured by a DMA4500 densitometer (Anto Paar) at $20 \text{ }^\circ\text{C}$. The value of v was 0.85 mL g^{-1} , which is close to the value ($v = 0.87 \text{ mL g}^{-1}$) reported by Chen *et al.*²⁸ As the partial specific volume usually does not have molecular weight dependence, we used this value for all of the PEtOx fractions.²⁶

Results and discussion

It is known that narrowly distributed linear poly(2-ethyl-2-oxazoline) with molecular weights ranging from 1 to $\sim 50 \text{ kg mol}^{-1}$ can be synthesized by conventional thermal heating and microwave-assisted cationic ring-opening polymerization

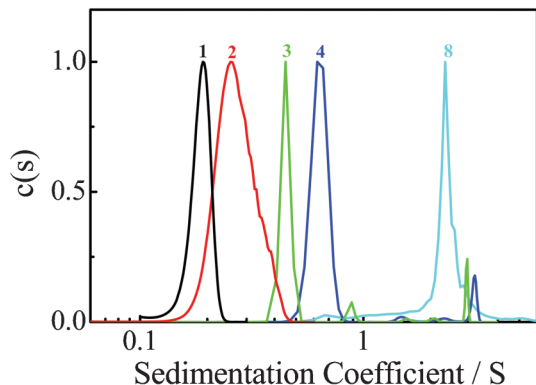


Fig. 2 Sedimentation coefficient (s) distributions of PETox-1, PETox-2, PETox-3, PETox-4, and PETox-8 at 20 °C, where the corresponding concentrations of the samples are 0.6 mg mL⁻¹, 0.6 mg mL⁻¹, 0.2 mg mL⁻¹, 0.3 mg mL⁻¹ and 0.5 mg mL⁻¹, respectively.

(CROP).^{11,29–33} However, it is still difficult to obtain narrowly distributed linear PETox with a molecular weight greater than 50 kg mol⁻¹. Our preliminary results showed that the distribution of the PETox samples fractionated by the dissolution–precipitation process in a mixture of dry THF and dry *n*-hexane were not narrow enough for AUC experiments.³⁴ Thus, in this study we used GPC to fractionate a commercial linear PETox sample. Owing to the advantage of AUC experiments that only small amounts of PETox samples (~0.2 mg) are needed, here only analytical GPC was used. Two PETox samples with molecular weights of 1.3 kg mol⁻¹ and 3.3 kg mol⁻¹ were synthesized by conventional thermal heating CROP.

Fig. 2 shows the sedimentation coefficient distributions of five PETox fractions in aqueous solution, analyzed with the continuous $c(s)$ distribution model by SEDFIT software. From Fig. 2, we know that the distributions of all of the fractions are narrow. Note that for the PETox-3 and PETox-4 fractions, small amounts of polymers with higher sedimentation coefficients exist in each fraction. This means that the polymers with a higher s , which may have the same hydrodynamic radius as the majority of the fractions, can not be fractionated by GPC.

Besides using the $c(s)$ model, the $c(s, f\bar{f}0)$ model has also been used to analyze the data.²⁷ Note that from the $c(s, f\bar{f}0)$ model, the polydispersity index (M_w/M_n) can be obtained. The corresponding results are summarized in Table 1. From Table 1, we know that the difference between the M_w values from these two models is less than 10% and the distributions of all of the fractions are narrow.

Due to solute–solute interactions and the shapes of the macromolecules differing from spherical, the hydrodynamic parameters (such as the sedimentation coefficient and hydrodynamic radius) may have a concentration dependence. In order to eliminate this effect, the concentration dependence of sedimentation coefficient and hydrodynamic radius was investigated. Because of the limited amount of the PETox fractions, less than 1 mg, the concentration of the PETox solutions can not be determined by a conventional balance. As

Table 1 Characterization of the PETox samples used

Sample	M_w (g mol ⁻¹)		M_w/M_n^a
	$c(s)^b$	$c(s, f\bar{f}0)$	
PETox-1	1300	1190	1.01
PETox-2	3230	3470	1.10
PETox-3	6890	7470	1.04
PETox-4	14 300	15 300	1.14
PETox-5	25 300	26 850	1.17
PETox-6	53 600	57 620	1.21
PETox-7	125 600	131 200	1.47
PETox-8	313 100	277 000	1.58

^a Analyzed by the $c(s, f\bar{f}0)$ model. ^b The relative error of the M_w is $\pm 3\%$.

we used interference optics as the detector and a triggerable laser diode as the light source, the relationship between the shift of the interference fringes (J) and the concentration of the solution (C) can be described as³⁵

$$J = \frac{a(dn/dC)}{\lambda} C \quad (2)$$

where a is the thickness of the centerpiece, dn/dC is the specific refractive index increment of the PETox polymer and λ is the wavelength of light in a vacuum. In this study, $a = 12$ mm and $\lambda = 660$ nm. The dn/dC value of the commercial linear PETox with a molecular weight of 500 000 g mol⁻¹ is (0.161 \pm 0.001) mL g⁻¹, which is the same as the value reported by Bijsterbosch *et al.*^{36,37} Based on the fact that dn/dC is independent of the molecular weight, this value can be used for all of the fractions.³⁶ Thus during our experiments, knowing the shift of the fringes will help us to determine the concentration of PETox, *i.e.* a concentration of 1 mg mL⁻¹ corresponds to 2.93 fringes.

From Fig. 3 and Fig. 4, we know that when the molecular weight is below $\sim 5 \times 10^4$ g mol⁻¹, both s and R_h do not change with concentration, and the extrapolation of s and R_h to zero concentration leads to s_0 and $R_{h,0}$ at infinite dilution. Note that Luo *et al.* reported that for PEG, when the molecular weight is less than 6×10^3 g mol⁻¹, s shows no dependence

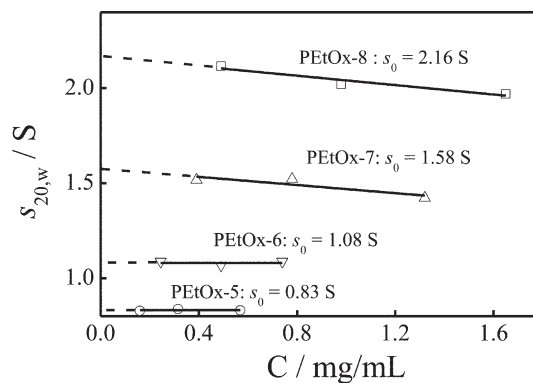


Fig. 3 Concentration dependence of the sedimentation coefficients of PETox-5, PETox-6, PETox-7 and PETox-8 at 20 °C.

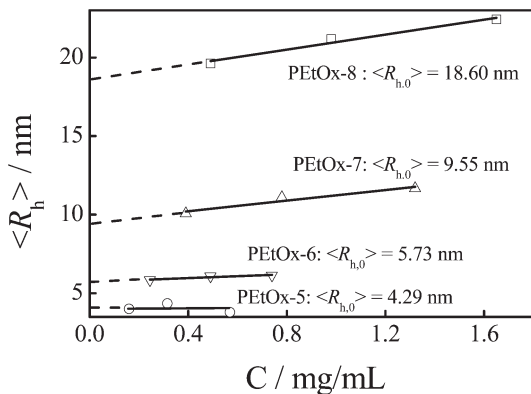


Fig. 4 Concentration dependence of the hydrodynamic radius of PETox-5, PETox-6, PETox-7 and PETox-8 at 20 °C.

on molecular weight.³⁸ The difference between these two polymers implies that for the same molecular weight, the interactions between PEG molecules are larger than that between PETox molecules, which is possibly due to the larger hydrodynamic volume of PEG.¹²

Besides sedimentation velocity (SV) experiments, we also used a combination of static and dynamic light scattering to characterize the PETox aqueous solutions. Fig. 5 shows that the intensity–intensity time correlation functions of the PETox-2 aqueous solution contains two relaxation modes. The faster mode corresponds to the pure diffusion of single PETox-2 chains and the slower relaxation mode may be related to the loosely-assembled aggregates due to the remaining hydrophobic tosyl end group. Our results show that the slow mode can be removed by repeated filtration for 2 h. Note that it is important to remove the slow mode for the measurement of the molecular weight and the hydrodynamic radius of PETox, especially for the PETox samples with smaller M_w . In our study, the same process was used for the characterization of two synthesized samples, PETox-1 and PETox-2.

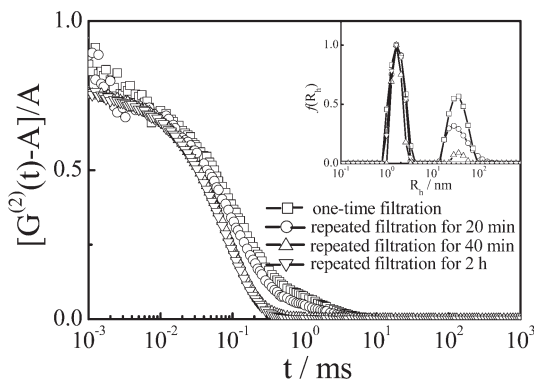


Fig. 5 A typical measured intensity–intensity time correlation function $[G^{(2)}(t, q) - A] / A$ for PETox-2 fraction aqueous solutions by one-time filtration and repeated filtration for different times. The inset shows the corresponding hydrodynamic radius distribution $f(R_h)$.

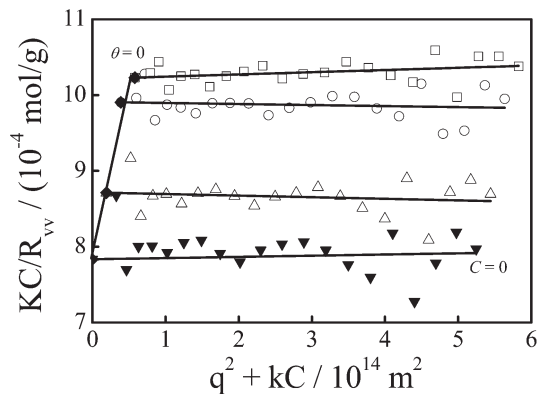


Fig. 6 A typical Zimm plot of PETox-1 in aqueous solution at 20 °C, where C is 19.5 mg mL⁻¹, 39 mg mL⁻¹ and 58 mg mL⁻¹, respectively.

Fig. 6 and Fig. 7 show typical Zimm plots and the hydrodynamic radius distribution of PETox-1, respectively. The extrapolation of $[KC/R_{wv}(q)]$ to $C \rightarrow 0$ and $q \rightarrow 0$ leads to a value of $M_w = 1.27 \times 10^3 \text{ g mol}^{-1}$ which is close to the value of $M_w = 1.30 \times 10^3 \text{ g mol}^{-1}$ determined by the SV experiments. The slope for the line plotting $[KC/R_{wv}(q)]_{q \rightarrow 0}$ versus C gives the value of $A_2 = (2.2 \pm 0.7) \times 10^{-3} \text{ mol mL g}^{-2}$, indicating that water is a good solvent for PETox. Due to the small size of PETox-1 in comparison with the wavelength of the laser light, there is no angular dependence of $[KC/R_{wv}(q)]$. Thus it is difficult to obtain a reliable $\langle R_g \rangle$ of PETox-1. The distribution of the hydrodynamic radius shows that PETox-1 is narrowly distributed and $\langle R_h \rangle = 1.02 \text{ nm}$, which is also consistent with the value determined by the SV experiments ($\langle R_h \rangle = 0.95 \text{ nm}$). Note that the scattering light intensity is proportional to the square of the mass of a single scattering object. In order to obtain a large enough scattering light intensity, $\sim 500 \text{ mg}$ of PETox-1 was needed to determine the accurate molecular weight and R_h , as the molecular weight of PETox-1 is as small as $\sim 1.3 \times 10^3 \text{ g mol}^{-1}$.

Fig. 8 shows that there is a scaling relationship between $s_{20,w}$ and M_w when M_w is in the range of $1 \times 10^3 \text{ g mol}^{-1}$ and 4

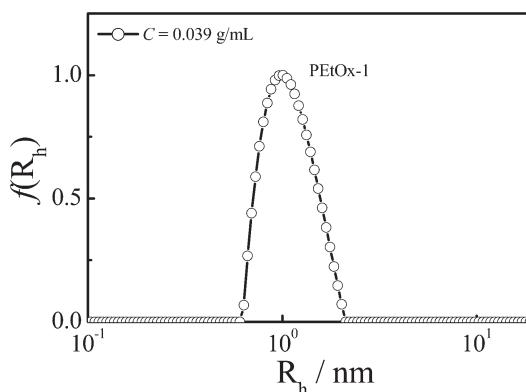


Fig. 7 Hydrodynamic radius distribution of PETox-1 in aqueous solution, where C is 39 mg mL⁻¹.

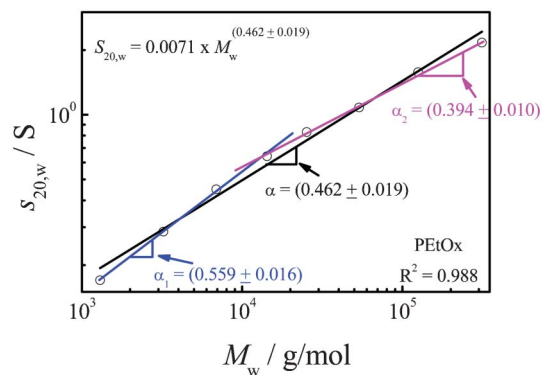


Fig. 8 Weight average molecular weight dependence of sedimentation coefficient ($s_{20,w}$) at 20 °C. The relative error of $s_{20,w}$ is $\pm 5\%$.

$\times 10^5 \text{ g mol}^{-1}$, *i.e.* $s_{20,w} = K_s \times M_w^\alpha = 0.0068 \text{ (S)} \times M_w^{0.462 \pm 0.019}$. The scaling index is $\alpha = (0.462 \pm 0.019)$, which is between 0.4 and 0.5, indicating that PEtOx polymers adopt a random coil conformation in aqueous solution.³⁹ Luo *et al.* reported that for PEG, the sedimentation coefficient (S_0) scales to M_w as $s_{20,w} = K_s \times M_w^\alpha = 0.0061 \text{ (S)} \times M_w^{0.469 \pm 0.008}$.³⁸ The scaling index α for PEtOx is similar to that of PEG, implying that both of the polymers adopt the same conformation in water. Fig. 8 also shows a transition of the scaling laws. The results show that values of $\alpha_1 = 0.559 \pm 0.016$ and $\alpha_2 = 0.394 \pm 0.010$ were obtained for $M_w < 2 \times 10^4 \text{ g mol}^{-1}$ and $2 \times 10^4 \text{ g mol}^{-1} < M_w < 4 \times 10^5 \text{ g mol}^{-1}$, respectively. It should be noted that the scaling index is typically around 0.67 for a compact sphere, 0.4–0.5 for a random coil and 0.15 for a rigid rod.⁴⁰ The parameters from the five samples with higher M_w are lower than the four samples with lower M_w , indicating that the PEtOx samples with higher M_w adopt a more extended coil conformation.

Both Chen *et al.* and Ambreen *et al.* studied the phase transition of the PEtOx aqueous solution by laser light scattering.^{34,41} Chen *et al.* reported that the $\langle R_h \rangle$ of PEtOx polymer with a molecular weight of $1.16 \times 10^5 \text{ g mol}^{-1}$ was 10.7 nm at 30 °C which was lower than its cloud point.⁴¹ Ambreen *et al.* characterized a narrowly distributed PEtOx fraction by a combination of static and dynamic light scattering and showed that the $\langle R_h \rangle$ of this fraction with a M_w of $8.7 \times 10^5 \text{ g mol}^{-1}$ was 29 nm.³⁴ We have combined their data together with our data in this study in Fig. 9 to show the molecular weight dependence of R_h . From Fig. 9, we know that $R_{h,0} = K_{R_{h,0}} \times M_w^\beta = 0.0179 \text{ (nm)} \times M_w^{0.539 \pm 0.012}$. Note that for real polymer chains in a good solvent and a theta solvent, the scaling indexes are 0.59 and 0.5, respectively.⁴² Recently, using a coarse-grained molecular dynamics simulation, Wang *et al.* reported that the radius of gyration of poly(ethylene terephthalate) scales with the degree of polymerization with a scaling index of 0.50, which is very close to the theoretical value. The scaling index obtained in our study is between the values predicted for in the good solvent and the theta solvent.^{43–45}

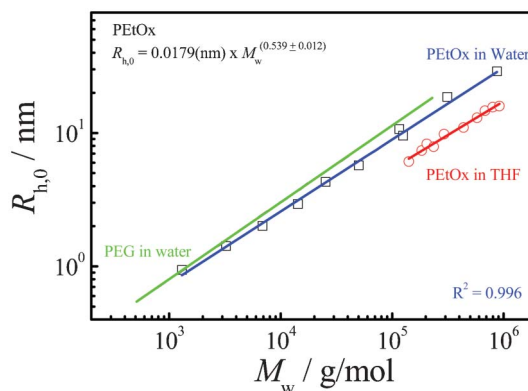


Fig. 9 Weight average molecular weight (M_w) dependence of the hydrodynamic radius ($R_{h,0}$) of PEtOx at 20 °C. The hydrodynamic radius of PEG in aqueous solution (green line) and PEtOx in THF (red line) were taken from ref. 38 and 21. The relative error of $R_{h,0}$ is $\pm 2\%$.

Moreover, the sum of α and β is 1.001, which is reasonable because from the Svedberg equation we know that $M^1 \propto s/D \propto s \cdot R_h \propto (K_s \cdot M^\alpha) \times (K_{R_{h,0}} \cdot M^\beta) \propto (K_s \cdot K_{R_h}) \times M^{\alpha+\beta}$. Fig. 9 also shows the weight-average molecular weight dependence of the hydrodynamic radius of PEG in water and PEtOx in THF. For the same molecular weight of PEtOx and PEG, the hydrodynamic radius of PEG is higher than that of PEtOx. Based on their structures, as shown in Fig. 1, the reason that PEG has a higher hydrodynamic radius may be due to its more favorable interaction with water molecules, and a larger degree of polymerization because the repeating unit of PEG has a smaller molar mass. Moreover, it is obvious that water is a better solvent for PEtOx than THF because for the same M_w , the R_h in water is much larger than that in THF. Knowing the scaling law between R_h and molecular weight can help us to choose PEtOx polymers with an appropriate molecular weight. For example, Armstrong stated that nonionic polymers with a R_h less than 4 nm can inhibit red blood cell aggregation and those with a R_h larger than 4 nm can enhance the aggregation.¹⁹ Based on Fig. 9, we know that the R_h of a PEtOx polymer with a molecular weight of $2.3 \times 10^4 \text{ g mol}^{-1}$ is 4 nm. Furthermore, if we consider that the interactions between PEtOx and proteins is similar to those between PEG and proteins, we can replace PEG with PEtOx of the same hydrodynamic radius, according to the scaling laws between the R_h and M_w of the two polymers. For instance, for three approved PEG conjugates (PEG-growth hormone receptor antagonist, PEG-interferon $\alpha 2b$ and Pegfilgrastim), PEG polymers with molecular weights of $5 \times 10^3 \text{ g mol}^{-1}$, $1.2 \times 10^4 \text{ g mol}^{-1}$ and $2 \times 10^4 \text{ g mol}^{-1}$ have been used.⁵ We could choose PEtOx polymers which have the same R_h to replace the PEG polymers, that is, the corresponding molecular weights of PEtOx are $6.5 \times 10^3 \text{ g mol}^{-1}$, $1.7 \times 10^4 \text{ g mol}^{-1}$ and $2.8 \times 10^4 \text{ g mol}^{-1}$, respectively.

Conclusion

By the use of a combination of analytical ultracentrifugation and laser light scattering, the relationships between the hydrodynamic radius ($R_{h,0}$), the sedimentation coefficient ($s_{20,w}$) at infinite dilution and the molecular weight of a series of linear poly(2-ethyl-2-oxazoline) polymers in aqueous solution have been studied. Our results show that $R_{h,0}$ and $s_{20,w}$ scale with molecular weight (M_w) as $R_{h,0} = K_{R_{h,0}} \times M_w^\beta = 0.0179$ (nm) $\times M_w^{0.539 \pm 0.012}$ and $s_{20,w} = K_s \times M_w^\alpha = 0.0071$ (S) $\times M_w^{0.462 \pm 0.019}$, respectively, indicating that PETox polymers adopt a random coil conformation in aqueous solution. Our findings will provide a guide for choosing PETox polymers with an appropriate molecular weight for its pharmaceutical applications.

Acknowledgements

The financial support of the National Program on Key Basic Research Project (2012CB933802), the National Natural Scientific Foundation of China (NNSFC) Projects (21274140), and the Scientific Research Foundation for the Returned Overseas Chinese Scholars, State Education Ministry is gratefully acknowledged.

References

- 1 B. Jeong, Y. H. Bae and S. W. Kim, *Macromolecules*, 1999, **32**, 7064.
- 2 M. J. Roberts, M. D. Bentley and J. M. Harris, *Adv. Drug Delivery Rev.*, 2002, **54**, 459.
- 3 J. M. Harris and R. B. Chess, *Nat. Rev. Drug Discovery*, 2003, **2**, 214.
- 4 P. Caliceti, *Adv. Drug Delivery Rev.*, 2003, **55**, 1261.
- 5 F. M. Veronese and G. Pasut, *Drug Discovery Today*, 2005, **10**, 1451.
- 6 T. C. Fisher, J. K. Armstrong, R. B. Wenby, H. J. Meiselman, R. Leger and G. Garratty, *Blood*, 2003, **102**, 559a.
- 7 J. K. Armstrong, R. Leger, R. B. Wenby, H. J. Meiselman, G. Garratty and T. C. Fisher, *Blood*, 2003, **102**, 556a.
- 8 J. K. Armstrong, G. Hempel, S. Kolling, L. S. Chan, T. Fisher, H. J. Meiselman and G. Garratty, *Cancer*, 2007, **110**, 103.
- 9 S. Zalipsky, C. B. Hansen, J. M. Oaks and T. M. Allen, *J. Pharm. Sci.*, 1996, **85**, 133.
- 10 S. C. Lee, Y. K. Chang, J. S. Yoon, C. H. Kim, I. C. Kwon, Y. H. Kim and S. Y. Jeong, *Macromolecules*, 1999, **32**, 1847.
- 11 F. Wiesbrock, R. Hoogenboom, M. A. M. Leenen, M. A. R. Meier and U. S. Schubert, *Macromolecules*, 2005, **38**, 5025.
- 12 T. X. Viegas, M. D. Bentley, J. M. Harris, Z. F. Fang, K. Yoon, B. Dizman, R. Weimer, A. Mero, G. Pasut and F. M. Veronese, *Bioconjugate Chem.*, 2011, **22**, 976.
- 13 R. Hoogenboom, F. Wiesbrock, H. Huang, M. A. M. Leenen, H. M. L. Thijs, S. F. G. M. van Nispen, M. van der Loop, C.-A. Fustin, A. M. Jonas, J.-F. Gohy and U. S. Schubert, *Macromolecules*, 2006, **39**, 4719.
- 14 N. Adams and U. S. Schubert, *Adv. Drug Delivery Rev.*, 2007, **59**, 1504.
- 15 R. Hoogenboom, *Macromol. Chem. Phys.*, 2007, **208**, 18.
- 16 A. Mero, G. Pasut, L. D. Via, M. W. M. Fijten, U. S. Schubert, R. Hoogenboom and F. M. Veronese, *J. Controlled Release*, 2008, **125**, 87.
- 17 R. Hoogenboom, *Angew. Chem., Int. Ed.*, 2009, **48**, 7978.
- 18 Z. Ota, H. Makino, Y. Takaya and T. Ofuji, *Renal Physiol.*, 1980, **3**, 317.
- 19 J. K. Armstrong, R. B. Wenby, H. J. Meiselman and T. C. Fisher, *Biophys. J.*, 2004, **87**, 4259.
- 20 S. L. Sim, T. He, A. Tscheliessnig, M. Mueller, R. B. Tan and A. Jungbauer, *J. Biotechnol.*, 2012, **157**, 315.
- 21 J. H. Sung and D. C. Lee, *Polymer*, 2001, **42**, 5771.
- 22 B. H. Zimm, *J. Chem. Phys.*, 1948, **16**, 1099.
- 23 B. Chu, *Laser Light Scattering*, Academic Press, New York, 1991.
- 24 C. Wu and K. Q. Xia, *Rev. Sci. Instrum.*, 1994, **65**, 587.
- 25 B. Berne and R. Pecora, *Dynamic Light Scattering*, Plenum Press, New York, 1976.
- 26 P. Schuck, *Biophys. J.*, 2000, **78**, 1606.
- 27 P. H. Brown and P. Schuck, *Biophys. J.*, 2006, **90**, 4651.
- 28 C. H. Chen, J. Wilson, W. Chen, R. M. Davis and J. S. Riffle, *Polymer*, 1994, **35**, 3587.
- 29 O. Sedlacek, B. D. Monnery, S. K. Filippov, R. Hoogenboom and M. Hruby, *Macromol. Rapid Commun.*, 2012, **33**, 1648.
- 30 F. Wiesbrock, R. Hoogenboom, C. H. Abeln and U. S. Schubert, *Macromol. Rapid Commun.*, 2004, **25**, 1895.
- 31 F. Wiesbrock, R. Hoogenboom and U. S. Schubert, *Macromol. Rapid Commun.*, 2004, **25**, 1739.
- 32 R. Hoogenboom and U. S. Schubert, *Macromol. Rapid Commun.*, 2007, **28**, 368.
- 33 C. Guerrero-Sanchez, R. Hoogenboom and U. S. Schubert, *Chem. Commun.*, 2006, 3797.
- 34 J. Ambreen, J. X. Yang, X. D. Ye and M. Siddiq, *Colloid Polym. Sci.*, 2013, **291**, 919.
- 35 W. Machtle and L. Borger, *Analytical Ultracentrifugation of Polymers and Nanoparticles*, Springer, Berlin, Heidelberg, New York, 2006.
- 36 H. D. Bijsterbosch, M. A. Cohen Stuart, G. J. Fleer, P. van Caeter and E. J. Goethals, *Macromolecules*, 1998, **31**, 7436.
- 37 H. D. Bijsterbosch, M. A. Cohen Stuart and G. J. Fleer, *Macromolecules*, 1998, **31**, 9281.
- 38 Z. L. Luo and G. Z. Zhang, *J. Phys. Chem. B*, 2009, **113**, 12462.
- 39 S. E. Harding, *Biophys. Chem.*, 1995, **55**, 69.
- 40 S. Hokputsa, K. Jumel, C. Alexander and S. E. Harding, *Carbohydr. Polym.*, 2003, **52**, 111.
- 41 F. P. Chen, A. E. Ames and L. D. Taylor, *Macromolecules*, 1990, **23**, 4688.
- 42 I. Teraoka, *Polymer Solutions: An Introduction to Physical Properties*, John Wiley & Sons, Inc., New York, 2002.
- 43 Q. Wang, D. J. Keffer, D. M. Nicholson and J. B. Thomas, *Macromolecules*, 2010, **43**, 10722.
- 44 Q. Wang, D. J. Keffer and D. M. Nicholson, *J. Chem. Phys.*, 2011, **135**, 214903.
- 45 Q. Wang, D. J. Keffer, S. Deng and J. Mays, *J. Phys. Chem. C*, 2013, **117**, 4901.